AIP Conference Proceedings

Search for two-proton radioactivity of ^{19}Mg in a tracking experiment

Cite as: AIP Conference Proceedings **961**, 93 (2007); https://doi.org/10.1063/1.2827290
Published Online: 03 December 2007

I. Mukha, K. Sümmerer, L. Acosta, M. A. G. Alvarez, E. Casarejos, A. Chatillon, D. Cortina-Gil, J. Espino, A. Fomichev, J. E. García-Ramos, H. Geissel, J. Gómez-Camacho, L. Grigorenko, J. Hoffmann, O. Kiselev, A. Korsheninnikov, N. Kurz, Yu. Litvinov, I. Martel, C. Nociforo, W. Ott, M. Pfutzner, C. Rodríguez-Tajes, E. Roeckl, M. Stanoiu, H. Weick, and P. J. Woods


View Online

Export Citation

ARTICLES YOU MAY BE INTERESTED IN

Study Of The Scattering Of Halo Nuclei Around The Coulomb Barrier
AIP Conference Proceedings **1336**, 570 (2011); https://doi.org/10.1063/1.3586166

Radia2: A new tool for radiotherapy verification
AIP Conference Proceedings **1541**, 183 (2013); https://doi.org/10.1063/1.4810838

Scattering of ^{8}He on ^{208}Pb at 22 MeV
AIP Conference Proceedings **1541**, 175 (2013); https://doi.org/10.1063/1.4810834

AIP Publishing

AIP Conference Proceedings

Lock-in Amplifiers
up to 600 MHz
Watch

AIP Publishing

AIP Conference Proceedings **961**, 93 (2007); https://doi.org/10.1063/1.2827290

© 2007 American Institute of Physics.

Search for two-proton radioactivity of ^{19}Mg in a tracking experiment

I. Mukha[*,†], K. Sümmerer[**], L. Acosta[‡], M. A. G. Alvarez[*], E. Casarejos[§], A. Chatillon[**], D. Cortina-Gil[§], J. Espino[*], A. Fomichev[¶], J. E. García-Ramos[‡], H. Geissel[**], J. Gómez-Camacho[*], L. Grigorenko[¶,**], J. Hoffmann[**], O. Kiselev[**,‖], A. Korsheninnikov[†], N. Kurz[**], Yu. Litvinov[**], I. Martel[‡], C. Nociforo[**], W. Ott[**], M. Pfutzner[††], C. Rodríguez-Tajes[§], E. Roeckl[**], M. Stanoiu[**,‡‡], H. Weick[**] and P. J. Woods[§§]

[*]*Universidad de Sevilla, ES-41012 Seville, Spain*
[†]*RRC "Kurchatov Institute", RU-123184 Moscow, Russia*
[**]*Gesellschaft für Schwerionenforschung, D-64291 Darmstadt, Germany*
[‡]*Universidad de Huelva, ES-21071 Huelva, Spain*
[§]*Universidade de Santiago de Compostela, ES-15782 Santiago de Compostela, Spain*
[¶]*Joint Institute for Nuclear Research, RU-141980 Dubna, Russia*
[‖]*Johannes Gutenberg Universität, D-55099 Mainz, Germany*
[††]*IEP, Warsaw University, PL-00681 Warszawa, Poland*
[‡‡]*IFIN-HH, P. O. BOX MG-6, Bucharest, Romania*
[§§]*University of Edinburgh, EH1 1HT Edinburgh, UK*

Abstract. The two-proton radioactivity of the previously unknown ^{19}Mg ground-state is observed by tracking the decay products in-flight. The trajectories of the 2p-decay products, ^{17}Ne+p+p, have been measured by using tracking micro-strip detectors which allowed to reconstruct the 2p-decay vertices and fragment correlations. The half-life of ^{19}Mg deduced from the measured vertex distribution is 4.0(15) ps in the system of ^{19}Mg. The Q-value of the 2p-decay of the ^{19}Mg ground-state inferred from the measured p–p–^{17}Ne correlations is 0.75(5) MeV.

Keywords: radioactivity; measured direct two-proton decay of ^{19}Mg [from ^{24}Mg fragmentation and subsequent ^{20}Mg neutron knock-out]; measured Q_{2p}, $T_{1/2}$. Three-body model calculations.
PACS: 21.10.-k; 21.10.Tg; 21.45.+v; 23.50.+z

Introduction. Two-proton (2p) radioactivity, a spontaneous decay of an atomic nucleus by the emission of two protons, is the most recently discovered nuclear disintegration mode. This phenomenon was predicted for a number of proton-rich isotopes that have an even number of protons and lie beyond the proton drip-line [1]. The 2p radioactivity has first been reported for ^{45}Fe with a half-life ($T_{1/2}$) of about 4 ms, which is about 1000 times longer than the quasi-classical estimate of "di-proton" (or ^{2}He-cluster) emission [2, 3]. Further observations of 2p radioactivity reported for ^{54}Zn [4], ^{94m}Ag [5] have confirmed unexpectedly large $T_{1/2}$ values of 2p precursors. The recently-developed first quantum-mechanical theory of 2p-radioactivity which uses a three-body "core"+p+p model [6, 7, 8] interprets this observation as being due to a considerable influence of Coulomb and centrifugal barriers together with nuclear structure effects, and is able to predict the regular existence of long-lived 2p precursors [7, 8]. Two-proton emission can

CP961, *Proton Emitting Nuclei and Related Topics –PROCON 2007*, edited by L. Ferreira and P. Arumugam
© 2007 American Institute of Physics 978-0-7354-0475-5/07/$23.00

also occur from short-lived nuclear resonances and excited states (see, e.g., [9, 10, 11]) where the mechanism of 2p emission may depend on the reaction populating the parent resonance, in contrast to 2p radioactivity. The inverse reaction to 2p decay, namely 2p capture, is expected to play an important role in the synthesis of heavy elements in the Universe, possibly bridging some "waiting points" in the "hot" rp-process, see e.g. [12]. The ^{19}Mg ground-state is a prospective candidate for the observation of 2p radioactivity by the in-flight method. The pioneering theoretical studies of the 2p-decay of ^{19}Mg in the framework of a three-body model [13] predict its half-life to be in the range from 0.5 to 60 ps and its 2p-decay energy from 0.55 to 0.85 MeV.

In-flight-decay experiment with tracking microstrip detectors. Experiments aimed at finding 2p radioactivity are based on implantation of the radioactive atoms and subsequent detection of their decay. This method is, however, limited to studies of nuclei with lifetimes larger than a few microseconds. We have performed an in-flight-decay experiment [14] in which all decay products are tracked and the decay vertices as well as the angular correlations of the decay products are deduced from the measured trajectories. Such a tracking technique is a precise and effective tool in high-energy physics. The basic idea underlying the in-flight 2p-decay experiment was suggested in Ref. [15] and discussed in detail in Ref. [13, 16]. The experimental setup is shown in Fig. 1. The ^{19}Mg ground-state can be produced in a one-neutron knock-out reaction from ^{20}Mg with the subsequent 2p decay populating ^{17}Ne+p+p. If the directions of the decay products are measured precisely, the vertex of each decay can be found as the point of closest approach of three fragment trajectories. If the half-life of ^{19}Mg is sufficiently long, a "delayed vertex" downstream from the target should show up. The half-life of ^{19}Mg can be derived by fitting the measured vertex distribution downstream from the target by an exponential function convoluted with the tracking detector resolution.

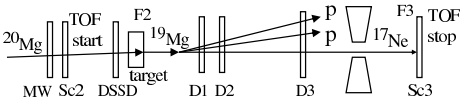

FIGURE 1. Sketch of the experimental set-up. The ^{20}Mg secondary beam was tracked by a silicon strip detector, DSSD, and a multiwire chamber, MW. ^{19}Mg nuclei were formed in the reaction (^{20}Mg,^{19}Mg)X and products of the decays ^{19}Mg$\rightarrow^{17}$Ne+p+p were tracked by three planes of silicon micro-strip detectors (D1–D3). ^{17}Ne ions were identified at foci F2 and F3 as described in the text.

The experiment was performed by using a 591*A* MeV beam of ^{24}Mg with an intensity of 10^9 s^{-1}, accelerated by the SIS facility at GSI, Darmstadt. The beam hit a primary 4 g/cm^2 thick ^{9}Be target at the entrance of the Projectile-Fragment Separator (FRS) [17] to produce a 450*A* MeV secondary beam of ^{20}Mg with an average intensity of 400 ions s^{-1} at the mid-plane F2 of the FRS where the secondary reaction (^{20}Mg,^{19}Mg) occurred in a second 2 g/cm^2 ^{9}Be target. Special magnetic optics settings were applied, the first half of the FRS being tuned in an achromatic mode using a wedge-shaped degrader, while its second half was set for identification of the heavy decay products, in particular ^{17}Ne, with high acceptance in angle and momentum. A micro-strip detector array [18], developed on the basis of the tracker of the AMS02 project [19], was positioned downstream of the secondary target. It consisted of 4 large-area (7x4 cm^2), 0.3 mm thick silicon micro-strip detectors with a pitch of 0.1 mm. They were used to

measure energy loss and positions of coincident hits of two protons and ^{17}Ne, allowing to reconstruct all fragment trajectories and derive the coordinates of the reaction vertex and angular proton-^{17}Ne correlations. The achieved transverse position accuracy is 40 μm for protons and 15 μm for ^{17}Ne. A double-sided Si strip detector (DSSD) and a multi-wire chamber (MW) were used upstream of the target for tracking the ^{20}Mg projectiles. The heavy-ions like ^{17}Ne were unambiguously identified by their time of flight (TOF) between foci F2 and F3, their magnetic rigidity and their energy deposition measured with the position-sensitive scintillator detectors Sc2 and Sc3 (see Fig. 1).

Results. Before discussing vertex distributions, we want to show how p–^{17}Ne angular correlations carry information on the decay energy. As depicted in Fig. 2a, the one-proton decay of a narrow state in a 1p-precursor leads to a characteristic angular correlation, with a peak appearing at an angle close to the largest possible one. Since the angles reflect the transverse proton momentum relative to ^{17}Ne, they are correlated with the decay energy. A similar effect is predicted for a direct 2p decay where the proton energy spectrum always has a relatively narrow peak centered close to half of the 2p-decay energy [13]. The angular correlations of each coincident proton with respect to the ^{17}Ne momentum, $\theta(p_1–^{17}Ne)–\theta(p_2–^{17}Ne)$, are shown in Fig. 2b. Most events fall into two distinct clusters: a spot around $\theta(p–^{17}Ne)$ of 30 mrad and a cross centered at 55 mrad. As will be discussed in more detail below, these two clusters can be attributed to the simultaneous 2p emission from the ^{19}Mg ground-state and to the sequential decay of excited states in ^{19}Mg via the ^{18}Na ground-state, respectively. We shall refer to these events as the "ground state" and "excited state", respectively.

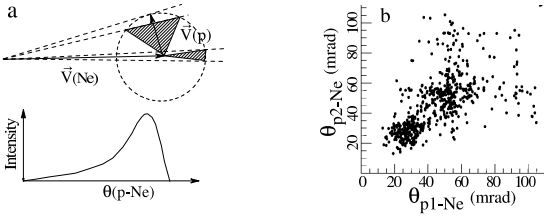

FIGURE 2. a) Illustration of the kinematical enhancement of angular correlations of decay products at the maximum possible angles between the decay products. b) Angular p–^{17}Ne correlations obtained from the measured ^{17}Ne+p+p events by selecting their vertex position inside the target (full circles).

We turn now to the discussion of decay vertex distributions. A sketch of two ideal vertex profiles is shown in Fig. 3a. The dissociation of ^{20}Mg into the non-resonant ^{17}Ne+p+p+n continuum should have a uniform distribution (grey curve) within the target. The same profile is expected if highly excited, short-lived states of ^{19}Mg are populated. The population of the ^{19}Mg ground-state and its subsequent (delayed) radioactive decay is expected to exhibit "grow-in" and "decay" curves along the beam direction corresponding to radioactivity (black line). The vertex profile in this case is expected to be broader and shifted downstream in comparison with the profile of prompt 2p emission. Due to the limited spatial resolution of the detectors and angular straggling of the fragments both idealized profiles are smeared in reality. Figures 3b and 3c show the experimental vertex profiles obtained from triple ^{17}Ne+p+p events gated by the conditions of "excited state" and "ground state" groups from Fig. 2b, respectively. These gates

are inferred from the respective angular p+^{17}Ne correlations as discussed below in the context of Fig. 4. We have performed Monte Carlo simulations [20] of vertex profiles for the 2p-decay ^{19}Mg$^{*}\rightarrow^{17}$Ne+p+p shown in Fig. 3b. The simulations assumed $T_{1/2}$=0 for the excited states of ^{19}Mg and took into account the above-mentioned experimental position accuracies in tracking the fragments in reconstructing the decay vertex coordinates. These simulations reproduce the data quantitatively. The vertex profile of the "excited state" in ^{19}Mg, where decays likely have $T_{1/2}$=0, serves as the reference case for estimating the position, width and uncertainty of the measured vertex distributions.

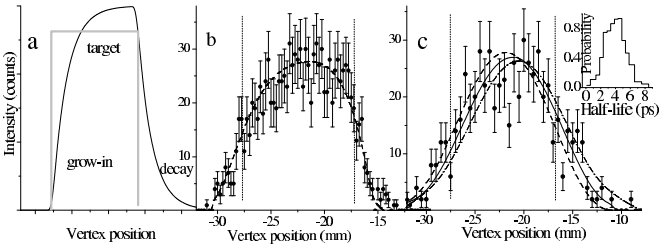

FIGURE 3. Profiles of the reaction vertices along the beam direction with respect to the closest microstrip detector. a) Ideal profiles of prompt (grey curve) and delayed (black curve) decays expected in a thick target. b) Vertex distribution of ^{17}Ne+p+p events gated by large p–^{17}Ne angles (and thus large p–^{17}Ne relative energies), which corresponds to short-lived excited states in ^{19}Mg (full circles with statistical uncertainties). The dashed curve shows the Monte Carlo simulations of the detector response for the 2p-decay ^{19}Mg$^{*}\rightarrow^{17}$Ne+p+p with $T_{1/2}$=0. c) The same as b) but gated by small p–^{17}Ne angles corresponding to the "ground state" group in Fig. 2b. The dashed curve depicts a simulation of the 2p-decay component with $T_{1/2}$=0. The solid and dash-dotted curves are fits to the data assuming a mixture of 25% of the $T_{1/2}$=0 component and 75% of the radioactivity component with $T_{1/2}$ 4 and 8 ps, respectively. The insert shows the probability (as a function of the assumed half-lives) that the simulations match the data.

The vertex profile in Fig. 3c accumulated under the condition that both protons originate from the "ground state" of ^{19}Mg has a broader distribution that is shifted in downstream direction by about 1 mm compared with the reference case shown in Fig. 3b. Its shape can be fitted by a simulation of the 2p decay of the ^{19}Mg ground-state by assuming a $T_{1/2}$=3.1(10) ps. However, the observed vertex profile cannot be related to the 2p decay of the ^{19}Mg ground-state alone. As will be discussed below, the events selected as representing the "ground state" decay actually contain contributions from both, the ground state and excited states of this nucleus. Therefore, using the angular-correlation data discussed below, we have applied a two-component fit of the observed vertex profile shown in Fig. 3c, with a mixture of 25% of the $T_{1/2}$=0 component and 75% of the component with $T_{1/2}$=4.0(15) ps. The corresponding fit describes the data quantitatively, i. e. with probability of about 95% that the data are compatible with the simulation histograms according to the standard statistical Kolmogorov test [21]. The uncertainty of this result is defined by the half-life range where the experimental data are described by the simulation with probability above 50%. The possible systematic uncertainty of $T_{1/2}$ due to the unknown shape of the $T_{1/2}$=0 background is estimated by another fit of the 2p-decay vertices gated by the condition that only one proton belongs to the "ground state" gate in Fig. 4b. In this case the $T_{1/2}$=0 component contributes by about 65%, and the derived $T_{1/2}$ value of ^{19}Mg amounts to $6(^{+2}_{-4})$ ps.

Figure 4 displays the angular p–^{17}Ne correlations derived from the coincident ^{17}Ne+p+p events. As we searched for a relatively long-lived radioactivity of ^{19}Mg, we

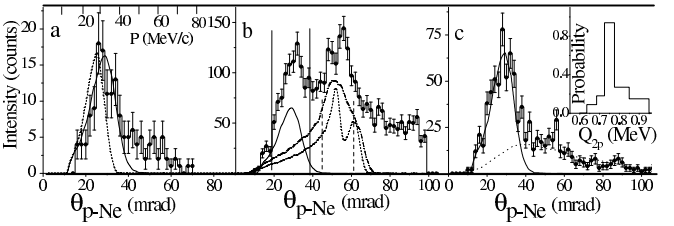

FIGURE 4. Angular p–^{17}Ne correlations obtained from the measured ^{17}Ne+p+p events (histograms with statistical uncertainties) obtained with three different gates: a) events with vertex positions between the target and the first detector. The solid and dashed curves show the simulations for the model calculations [13] of the ^{19}Mg 2p-decay with decay energies of 0.75 and 0.60 MeV, respectively. The upper axis shows a transverse momentum of proton relative to ^{17}Ne. b) Same as a) but gated on vertex positions inside the target. The solid curve is the same as in a). The dashed and dash-dotted curves illustrate the sequential proton emission of a suggested excited state in ^{19}Mg via a narrow and a broad (Γ=0.5 MeV) ground state of ^{18}Na, respectively. The vertical solid and dashed lines indicate the gates used for selecting vertex distributions for the "ground state" and "excited state" of ^{19}Mg, respectively (see text). c) Angular p_1-^{17}Ne correlations selected in the same way as in b) but additionally gated by a small angle in another p_2-^{17}Ne pair matching the "ground state" gate defined in b). The solid curve is identical to the one shown in a), the dotted curve is the fit of the broad distribution extrapolated into the "ground state" area. The insert shows the probability (as a function of 2p-decay energy) that the simulations match the data.

made two projections from the measured p–p–^{17}Ne correlations. One was gated on vertices downstream of the target where the radioactive decay of the ^{19}Mg ground-state should show up (Fig. 4a). The other distribution (Fig. 4b) was gated on vertices inside the target. The angular p–^{17}Ne correlations resulting from inside the target exhibit two peaks on top of a broad distribution while mostly one peak survives in the spectrum downstream from the target. The data are compared to simulations made for (i) the 2p-decay $^{19}\text{Mg}\rightarrow{}^{17}\text{Ne+p+p}$ according to the three-body model [13] and (ii) a sequential emission of protons from a suggested narrow state in ^{19}Mg via the ground state of ^{18}Na [22]. In both cases, the the 2p-decay energies were fitted to the peaks appearing in the experimental spectrum. The peak around 30 mrad was fitted by a Q_{2p} value of 0.75(5) MeV. In a similar way the peak around 55 mrad was fitted by assuming a sequential emission of about 1.8 MeV protons from an excited state in ^{19}Mg to the ground state of ^{18}Na and subsequently of 1.3 MeV protons, with a total Q_{2p} value of 3.2(2) MeV. Figure 4c shows the p_1-^{17}Ne correlations corresponding to the "ground state" peak in another pair p_2-^{17}Ne. The contribution from the "ground state" peak has the same shape as in Fig. 4b but the "excited state" peak is suppressed. This means that the "ground state" and "excited state" peaks cannot be explained by a sequential emission of protons from the same state in ^{19}Mg. The derived Q_{2p} value of 0.75 MeV matches the range of 2p-decay energies of 0.55–0.85 MeV predicted for ^{19}Mg [13] while a 2p-decay energy of about 3.2 MeV should result in immediate break-up regardless of the 2p-decay mechanism involved. Therefore the only plausible explanation of the p–^{17}Ne correlations observed inside and outside the target is that the 55 mrad peak can be ascribed to an excited state in ^{19}Mg, and the 30 mrad peak is related to the ^{19}Mg ground-state. In our procedure to determine the half-life of ^{19}Mg as described above,

we have used these two peaks as gates for producing the 2p-decay vertex distributions shown in Fig. 3. We should note that an unambiguous description of the 55 mrad "excited state" events is not possible yet.

Summary and outlook. The ground state in ^{19}Mg and its 2p radioactivity is observed with $T_{1/2}$=4.0(15) ps and Q_{2p}=0.75(5) MeV. The delayed 2p emission is manifested in the measured decay vertex profile and in the p–^{17}Ne correlations. The ^{19}Mg vertex profile is shifted respective the target center as expected for a short-lived radioactive nucleus. The p–^{17}Ne correlations display the ground and excited states of ^{19}Mg produced inside the target but only the ground state is seen outside the target area in downstream direction. The measured half-life and decay energy match the predictions of the three-body model while missing the predictions of the "di-proton" model by three orders of magnitude [13]. The method of measuring radioactivity in flight by precise tracking of all fragments with micro-strip detectors has proven to be a promising tool for systematic studies of 2p emitters predicted theoretically [8, 24].

Acknowledgments. The authors are indebted to M. Pohl and his co-workers of the DPNC, Universite de Geneve, for developing the micro-strip detectors. We appreciate in particular E. Cortina continuous support of this project. We thank A. Bruenle, K.H. Behr, W. Hueller, A. Kelic, A. Kiseleva, R. Raabe and O. Tarasov for their help during the preparations of the experiment. This work has been supported by contracts EURONS No. EC-I3 and FPA2003-05958, FPA2006-13807-C02-01 (MEC, Spain).

REFERENCES

1. V. I. Goldansky, *Nucl. Phys.* **19**, 482 (1960).
2. M. Pfutzner et al., *Eur. Phys. J. A* **14**, 279 (2002).
3. J. Giovinazzo et al., *Phys. Rev. Lett.* **89**, 102501 (2002).
4. B. Blank et al., *Phys. Rev. Lett.* **94**, 232501 (2005).
5. I. Mukha et al., *Nature (London)* **439**, 298 (2006).
6. L. V. Grigorenko et al., *Phys. Rev. Lett.* **85**, 22 (2000).
7. L. V. Grigorenko et al., *Phys. Rev. C* **64**, 054002 (2001).
8. L. V. Grigorenko and M. V. Zhukov, *Phys. Rev. C* **68**, 054005 (2003).
9. O. V. Bochkarev et al., *Nucl. Phys. A* **505**, 215 (1989).
10. R. A. Kryger et al., *Phys. Rev. Lett.* **74**, 860 (1995).
11. C. R. Bain et al.,*Phys. Lett. B* **373**, 35 (1996).
12. L. V. Grigorenko and M. V. Zhukov, *Phys. Rev. C* **72**, 015803 (2005).
13. L. V. Grigorenko, I. G. Mukha and M. V. Zhukov, *Nucl. Phys. A* **713**, 372 (2003).
14. I. Mukha et al., *Phys. Rev. Lett.* (2007), in print.
15. I. Mukha and G. Schrieder, *Nucl. Phys. A* **690**, 280c (2001).
16. I. Mukha, *Phys. Atomic Nuclei* **66**, 1519 (2003).
17. H. Geissel et al., *Nucl. Instrum. Methods Phys. Res. B* **70**, 286 (1992).
18. http://dpnc.unige.ch/ams/GSItracker/www/.
19. B. Alpat et al., *Nucl. Instrum. Methods Phys. Res. A* **540**, 121 (2005).
20. "GEANT - detector simulation tool", CERN software library, http://wwwinfo.cern.ch/asd/geant/.
21. W. T. Eadie et al., *"Statistical Methods in Experimental Physics",* North-Holland, 1971.
22. T. Zerguerras et al., *Eur. Phys. J. A* **20**, 389 (2004).
23. C. J. Woodward, R. E. Tribble and D. M. Tanner, *Phys. Rev. C* **27**, 27 (1983).
24. L. V. Grigorenko, I. G. Mukha and M. V. Zhukov, *Nucl. Phys. A* **714**, 425 (2003).